Article:
Menchicchi, B, Fuenzalida, JP, Hensel, A et al. (4 more authors) (2015) Biophysical Analysis of the Molecular Interactions between Polysaccharides and Mucin. Biomacromolecules, 16 (3). pp. 924-935. ISSN 1525-7797

https://doi.org/10.1021/bm501832y

Biophysical Analysis of the Molecular Interactions between Polysaccharides and Mucin

B. Menchicchi[a], J. P. Fuenzalida[a], A. Hensel[b], M. J. Swamy[c], L. David[d], C. Rochas[e], and F. M. Goycoolea[a]

[a)] Westfälische Wilhelms-Universität Münster, Institute of Plant Biology and Biotechnology (IBBP), Schlossgarten 3, 48149 - Münster, Germany goycoole@uni-muenster.de;

[b)]Westfälische Wilhelms-Universität Münster, Institute for Pharmaceutical Biology and Phytochemistry (IPBP), Hittorfstraße 56, D-48149 Münster, Germany

[c)] University of Hyderabad, School of Chemistry, - Hyderabad, Andra Pradesh, India;

[d)] University of Lyon, Laboratoire des Matériaux Polymères et des Biomatériaux-Boulevard A. Latarjet 15, 69622 Villeurbanne Cedex, France

[e)]CERMAV-CNRS, BP53, 3804, Grenoble, France

Abstract

Mucoadhesive materials adhere persistently to mucosal surfaces. A mucoadhesive delivery system could therefore facilitate the controlled release of drugs and optimize their bioavailability in mucosal tissues. Polysaccharides are the most versatile class of natural polymers for transmucosal drug delivery. We used microviscosimetry to explore the mucoadhesion of a library of polysaccharide families with diverse structural characteristics as a first step towards the rational design of mucoadhesive polysaccharide-based nanoformulations. Here we show that the magnitude of deviation between the viscosity of mixed polysaccharide–mucin solutions and the corresponding individual stock solutions can indicate underlying molecular interactions. We found that nonlinear monotonic curves predicted a correlation between the magnitude of interaction and the ability of polysaccharide coils to contract in the presence of salt (i.e. chain flexibility). Charge-neutral polysaccharides such as dextran and Streptococcus thermophilus exopolysaccharide did not interact with mucin. Synchrotron small-angle X-ray scattering (SAXS) data supported the previously described structural features of mucin. Furthermore, high-q scattering data (i.e. sensitive to smaller scales) revealed that when mucin is in dilute solution (presumably in an extended conformation) in the presence of low-Mw alginate, its structure resembles that observed at higher concentrations in the absence of alginate. This effect was less pronounced in the case of high-Mw alginate but the latter influenced the bulk properties of mucin–alginate mixtures (e.g. hydrodynamic radius and relative viscosity) more prominently than its low-Mw counterpart.

Figure for Table of Contents:

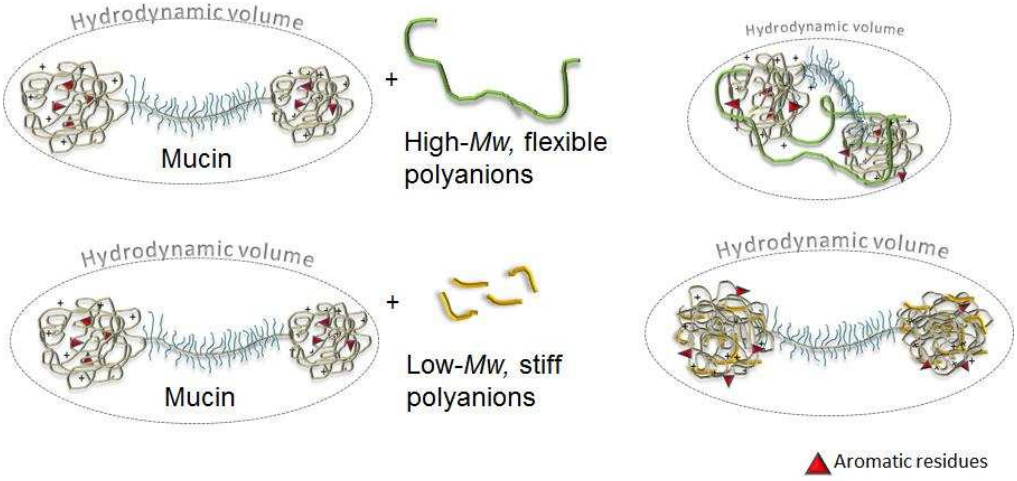

Introduction

The development of innovative nanomaterials for the targeted eradication of local bacterial infections requires functional building blocks that are biodegradable, biocompatible and non-toxic, and whose interactions with specific biological surfaces can be predicted and controlled. For mucosal delivery, materials can be designed to facilitate either mucoadhesion or mucopenetration,[1] but the short contact time with the gastrointestinal mucosa (8-10 h) limits the bioavailability of orally delivered drugs.[2] Mucoadhesive carriers therefore have the potential to prolong the controlled release of such drugs, increasing their bioavailability and enhancing the local transmucosal effect.[3] In contrast, mucopenetrating carriers promote drug transfer across the mucosal barrier quickly, thereby avoiding clearance caused by rapid turnover of the superficial layer.[4] Although a size-filtering mechanism regulated by mucin density determines whether carriers permeate or remain trapped, the mucin–carrier interaction is a key parameter that determines their fate.[5] Mucosal drug delivery vehicles that either penetrate rapidly or establish prolonged contact are difficult to develop because little is known about the interactions between mucin and other macromolecules.[6]

Many natural and synthetic polymers have mucoadhesive properties although the underlying mechanisms are not fully understood.[7] Several techniques have therefore been used to study the interactions between mucin and other materials in gels, solutions or in mucous tissues. We recently used a panel of biophysical techniques to study the interaction between chitosan and mucin in dilute solutions, focusing on the interacting forces and the intrinsic structure of the chitosan polymer.[8] We found that the mucoadhesive properties of chitosan were predominantly based on electrostatic interactions between positively-charged groups on the chitosan polymer and negatively-charged mucin, but that the molecular mass, conformation and overall flexibility of chitosan (the latter determined by the charge density, i.e. the degree of acetylation) also played a significant role.[8] However, negatively-charged polysaccharides such as alginates,[9] pectins[10] and poly(acrylic acid)[11] also show mucoadhesive properties, indicating that electrostatic interactions are not solely responsible. Mucin forms a complex macromolecular network carrying reactive functional groups (e.g. sialic acid) and intrinsic cross-linker residues (e.g. disulfide bonds), therefore offering many opportunities for interactions with the mucus layer including hydrogen bonding between sialic acids and carboxylate (e.g. alginate) or sulfate (e.g. dextran sulfate) residues, hydrophobic interactions with amino acids, and entanglement with hydrated, flexible polymers.

The diverse nature of polysaccharides and the lack of standardization among the techniques used to study mucoadhesion make it difficult to draw meaningful comparisons from the scientific literature. Some methods test for interactions directly at a macroscopic level (e.g. by measuring the force or

time required to detach a polymer from a mucin surface)[12] whereas others are based on the rheology of binary mixtures comprising different polymers in solution, allowing the synergy between two interacting molecules to be investigated by changes in viscosity.[13] Rheological synergism has been used to test the mucoadhesive properties of several polymers[13,14] including alginate[9] and chitosan.[15,16,17] One such study revealed negative synergy (i.e. a loss of viscosity)[16], or antagonism, when chitosan was mixed with mucin, whereas another by the same group found positive synergy (i.e. an increase in viscosity)[15] as also previously reported.[13] These discrepancies can be attributed to different experimental conditions, particularly the chitosan concentration[17] or mucin source, making direct comparisons challenging.[18] A standardized approach to the characterization of such interactions would therefore facilitate the rational selection of polysaccharides that are suitable for the design of mucoadhesive drug carriers.

Here we tested a series of polysaccharides differing in primary structure, molecular weight, charge density, conformation and (in the case of polyelectrolytes) the degree of coil contraction in the presence of salt, reflecting their intrinsic chain flexibility. We characterized the interactions between these polysaccharides and the soluble fraction of partially-purified porcine gastric mucin by microviscosimetry and in the case of alginate also investigated the molecular basis of such interactions using synchrotron small-angle X-ray scattering (SAXS). We were able to predict a correlation between the magnitude of interaction and the intrinsic contractibility of the polysaccharide coils. SAXS data derived from mucin–alginate mixtures at low concentrations showed that the presence of alginate induced the formation of a structure reminiscent of higher-concentration mucin solutions in the absence of alginate. These two behaviors may explain the synergy detected by microviscosimetry.

Materials and methods

Preparation of mucin and polysaccharide solutions

All polysaccharides were dissolved in milliQ water overnight by gentle stirring, and each solution was passed through a 5-µm disposable filter. The pH of the final solutions was adjusted to 4.5 with HCl or NaOH as appropriate. Two samples of pharmaceutical-grade chitosan – HMC^+15 (Mw ~27.5 kDa, DA = 14.8%) and HMC^+30 (Mw ~17 kDa, DA = 32.4%) – were purchased from HMC^+ (Halle, Saale Germany). Four additional forms of chitosan with high degrees of polymerization[19] were prepared from a parent sample provided by Mathani Chitosan Pvt. Ltd (Kerala, India): HDP 1 (Mw ~124 kDa, DA = 1.6%), HDP 11 (Mw ~122 kDa, DA = 11%), HDP 27 (Mw ~143 kDa, DA = 27.5%) and HDP 56 (Mw ~266 kDa, DA = 56%). The samples were dissolved in a 5% stoichiometric excess of HCl in ultrapure MilliQ water before filtration and pH adjustment as above.

We obtained dextran (Dex; Mw ~27.4 kDa), the two Leuconostoc spp. dextran sulfate sodium salts DexS40 (Mw ~49 kDa) and DexS500 (Mw ~632 kDa), sodium carboxymethylcellulose (CMC; Mw ~462 kDa), poly(acrylic acid) (PAA; Mw ~2651 kDa) and Streptococcus equi hyaluronic acid sodium salt (HA; Mw ~4585 kDa) from Sigma-Aldrich (Munich Germany). Fully characterized pectin (Pec25; Mw ~59.7 kDa, degree of etherification = 25.5%) and the alginates Alg400 (Mw ~406 kDa, M/G ratio = 0.95) and Alg4 (Mw ~4 kDa, M/G ratio = 1.42) were supplied and characterized by Danisco A/S (Tonder, Denmark).[20] S. thermophilus CRL 1190 exopolysaccharide (Eps; Mw ~1782 kDa) was isolated and characterized as previously described[21]. Xanthan (Xa; Mw ~625.9 kDa) and mesquite gum (MQ; Mw ~ 350 kDa) were samples prepared for earlier investigations.[22,23] The Mw of each polysaccharide was either determined experimentally by gel permeation chromatography/high-performance liquid chromatography (GPC–HPLC) with differential refractive index (DRI) multi-detection and a pullulan calibration curve or based on the values reported by the manufacturer or in previous studies (Figure 1). Porcine stomach mucin (type III, bound sialic acid 0.5–1.5%, partially-purified powder, batch no. 061M7006V) was purchased from Sigma-Aldrich and was prepared as previously described.[8]

De*termination of intrinsic viscosity and "degree of contraction"*

The dynamic viscosity of dilute polysaccharide solutions was measured using an AMVn automated rolling ball microviscosimeter (Anton Paar, Ostfildern, Germany) with a programmable tube angle based on the principle of the rolling ball time. The intrinsic viscosity [η] in water ($[\eta]_{H_20}$) and 0.1 M NaCl ($[\eta]_{NaCl}$), both at pH 4.5, was determined as previously described[8]. The degree of coil contraction was thus expressed as the following ratio: $[\eta]_{H_20}/[\eta]_{NaCl}$.

Preparation of polysaccharide–mucin mixtures

Stock solutions of polysaccharides and mucin closely matched in terms of relative viscosity (η_{rel} ~2) were mixed in different proportions to achieve composition ratios of the mucin mass fraction with respect to the total mass (denoted here as f) in the interval from f = 0 (i.e. only polysaccharide) to f = 1.0 (i.e. only mucin). The mixtures were allowed to equilibrate at 37°C shaking at 400 rpm for 20 min before commencing viscosity measurements.

Viscosity of mixed solutions

The dynamic viscosity of mixed polysaccharide–mucin solutions was measured as described above and the results were expressed as relative viscosity (η_{rel}). The deviation of η_{rel} between the mixtures and corresponding stock solutions was determined by adapting two previously-described methods.[24,13] A theoretical additive line (line of no interaction) was calculated from the sum of each individual contribution to the overall viscosity, which depended on their relative volumes at a given f mass ratio, according to the following equation:

$$\eta_{t(f)} = V_{p(f)}\,\eta_p + V_{m(f)}\,\eta_m \qquad \text{Eq. 1}$$

where $\eta_{t(f)}$ is the additive theoretical value of relative viscosity at a given value of f , $V_{p(f)}$ and $V_{m(f)}$ are the relative volumes in the mixture of polysaccharide and mucin, respectively, at a given value of f, and η_p and η_m are the relative viscosities of the stock solutions of polysaccharide and mucin, respectively. The difference between the experimental values (η_{exp}) of the mixtures and the corresponding theoretical values was then expressed as a percentage deviation from the theoretical additive line (Eq.2):

$$\%\ \text{deviation}_{(f)} = (\eta_{t(f)} - \eta_{exp(f)}) / \eta_{t(f)} \times 100 \qquad \text{Eq.2}$$

The integrated area under the curve (AUC) at different values of f was calculated from the sum of the trapezoids described by the experimental % deviation and the theoretical additive line values using Origin v8.5 (Origin Lab Corp., Northampton, MA).

Average size and zeta potential

The size distribution of mucin–alginate mixed solutions was determined by dynamic light scattering with non-invasive back scattering (DLS-NIBS) at an angle of 173° with an automatic attenuator setting. The electrophoretic mobility (μ_e) was determined by mixed-laser Doppler electrophoresis and phase analysis light scattering (M3-PALS). Both parameters were measured using a Malvern Zetasizer NANO-ZS (Malvern Instruments, Worcestershire, UK) equipped with a 4 mW He/Ne laser beam (λ = 633 nm). The ζ-potential of the various polysaccharides was obtained from the

electrophoretic mobility (μ_e) of the stock solutions of polysaccharides and mucin measured at pH 4.5 and 37°C using Henry's equation (Eq.3):

$$\mu e = \frac{(2\times\varepsilon\times\zeta\times f(Ka))}{3\eta} \qquad \text{Eq.3}$$

where f(Ka) is Smoluchowski's approximation (1.5), ε is the dielectric constant of the dispersant (water), and η is the viscosity of the solvent.

The size distributions of alginate–mucin (Alg4 and Alg400) mixtures were measured as described above. The mucin sample (5 mg/mL) was titrated as a function of pH using an MPT-2 autotitrator connected to a Malvern ZetasizerNano ZS (Malvern Instruments, UK). We recorded variations in the DLS-NIBS correlation functions and ζ-potential during titration with 1 M and 0.1 M HCl in the pH range 7–1.2.

Fluorescence quenching

Differences in the fluorescence emission spectra of mucin following the addition of different alginate samples were measured by placing 2 ml of 0.5 mg/mL mucin solution (in acetate buffer, pH 4.5) in a 1×1×4.5 cm quartz cell. This was the concentration required to achieve an absorbance of ~0.1 at 295 nm. We then added 20-μL aliquots of 5 mg/mL Alg4 and 2.5 mg/mL Alg400 (both prepared in acetate buffer, pH 4.5) and measured the fluorescence (λ_{ex} = 295 nm; λ_{em} = 338 nm) using a PC-1 fluorescence spectrometer from ISS (Champaign, IL, USA). The fluorescence was corrected for the background signal (water and alginate only) and by applying inner-filter correction. The quenching effect of alginate on mucin was evaluated by inspecting the fluorescence spectra and the Stern-Volmer curve F_0/F vs alginate concentration, where F and F_0 are the fluorescence of mucin in the presence and absence of alginate, respectively.

Synchrotron small-angle X-ray spectrometry

Synchrotron SAXS was use to characterize different concentrations of mucin (dissolved in water at pH 4.5) in the presence and absence of Alg4 and Alg400. The measurements were carried out at the European Synchrotron Research Facility (Grenoble, France) in beamline BM02 with the following settings: E = 16 kEv (λ = 0.0785 Å), sample-to-detector distance = 1.88 m. The collected scattering data were calibrated against the known positions of silver behenate powder Bragg reflections. The intensity values were corrected with respect to the relative dissolution medium (water, pH 4.5) and the scattered intensity versus q ($Å^{-1}$) was analyzed using OriginPro v8.5 software.

Results and discussion

We investigated the structure–function relationship underlying the interactions between a series of polysaccharides (general properties summarized in Table S1 in supporting information) and the soluble fraction of porcine stomach mucin using two different approaches. First, we considered solution properties such as intrinsic viscosity (in water and 0.1 M NaCl, [η]) and electrophoretic mobility (μ_ε) and we used microviscosimetry to measure changes in the viscosity of polysaccharide–mucin mixtures of different ratios compared to the individual stock solutions. We also considered the degree of contraction of the polysaccharide chains. Second, we used high-brilliance synchrotron SAXS and fluorescence spectroscopy to study the mechanism of interaction in two representative systems (Alg4–mucin and Alg400–mucin), one involving a loss of viscosity and the other a gain. The latter is observed only rarely in interactions between polysaccharides[25] and may therefore reflect the presence of specific linkages or polymer–mucin interactions. Recently, it has been documented increases in viscosity, elasticity and relaxation time, and changes in SANS scattering intensity, of mucin solutions upon addition of non-polysaccharide galloylated catechins (e.g. polyphenols) due to a cross-linking effect.[26,27]

Characterization of the polysaccharides

Most of the polysaccharides we tested are water-soluble polymeric macromolecules whose interactive properties therefore reflect a combination of forces that stabilize the structure of the macromolecule by controlling electrostatic repulsive and attractive forces, hydrophobic interpolymer interactions and the stiffness of the chain (defined by the persistence length, Lp).[28] Therefore, the intrinsic viscosity [η], or the hydrodynamic volume occupied by the polymer chain extrapolated at zero-concentration, correlates directly with the Mw (according to the Mark-Houwink equation) and the local stiffness of the ionic or neutral polymer chain. Stiffer polysaccharides such as alginate (Alg400) would thus show a higher intrinsic viscosity in water than more flexible molecules with a similar Mw, such as dextran sulfate (DexS500). The same comparison can be made between chitosan molecules with a high degree of polymerization but a low degree of acetylation (HDP 1) and those with a high degree of polymerization and a high degree of acetylation (HDP 56), and between pectin (Pec25) and dextran sulfate (DexS40) as shown in Figures 1a and 1b. Furthermore, the Lp and conformation of the chain is controlled by the ionic strength in solutions of charged polysaccharides.[29] Due to charge screening in the presence of 0.1 M NaCl, repulsive Coulombic forces have less impact on the conformation of the polymer, thus favoring interpolymer rather than polymer–solvent interactions.

The ability to adapt to environmental changes depends on the intrinsic flexibility of the chain and its Mw, and in most cases results in a substantial decline in the intrinsic viscosity.[30] This difference is more pronounced in synthetic polymers than natural polymers[31] thus explaining why PAA showed the largest $[\eta]_{H_2O}/[\eta]_{NaCl}$ ratio of 23.77, here described as the "degree of contraction" (Figure 1c and 1f). The ranking then continues with the high-Mw DexS500 (10.89), the high-Mw chitosan polymers HDP 11 and HDP 27 (4.59 and 4.49, respectively), Alg400 (4.65) and HA (4.39). The relatively low degree of contraction observed for Xa (2.75) reflects the rigid character of this macromolecule, which is known to undergo to ordered/disordered transition under certain temperature–ionic strength conditions.[32] Even lower values (~ 1.00) were observed for EPS1190 and Dex because they are not polyelectrolytes and therefore do not respond to ionic strength variations by undergoing a conformational change. In the case of Alg 4, the low degree of contraction (1.19) directly reflects its oligomeric nature (Mw ~4000, DP ~22).

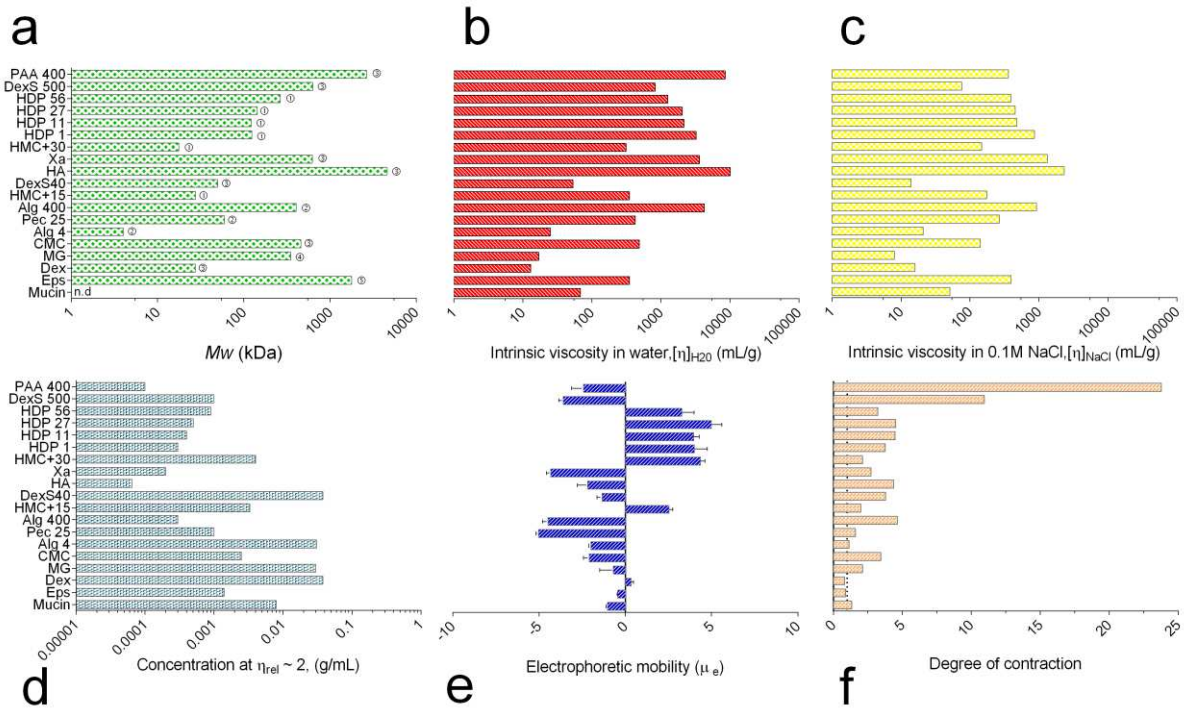

Figure 1. Physicochemical properties of the polysaccharides used in this investigation. PAA = poly(acrylic acid), DexS40 = low-Mw dextran sulfate, DexS500 = high-Mw dextran sulfate, HDP 1 = high-Mw chitosan (DA 1.6%), HDP 11 = high-Mw chitosan (DA 11%), HDP 27: = high-Mw chitosan (DA 27.5%), HDP 56 = high-Mw chitosan (DA 56%), HCM+30 = low-Mw chitosan (DA 32.4%), HCM+15 = low-Mw chitosan (DA 14.8%), Xa = xanthan, HA = hyaluronic acid, Alg 400 = high-Mw alginate, Alg 4 = low-Mw alginate, Pec 25 = pectin, CMC = carboxymethyl cellulose, MG = mesquite gum, Dex = dextran, Eps = exopolysaccharide from S. thermophilus CRL 1190. a) Mw determined as follows: ①, ④ and ⑤ from previous work[19,33,21], ② manufacturer's specifications, and ③determined by GPC-HPLC with DRI detection. b) Intrinsic viscosity in water (pH 4.5, 37°C). c) Intrinsic viscosity in 0.1 M NaCl (pH 4.5, 37°C). d) Concentration of stock

solution to achieve relative viscosity of ~2.0 in water (pH 4.5, 37°C). e) Electrophoretic mobility. f) Degree of contraction, calculated as the $[\eta]_{H_2O}/[\eta]_{NaCl}$ ratio.

Polysaccharide–mucin interactions determine viscosity synergism

Polysaccharide stock solutions (η_{rel} ~2) were mixed with mucin (8 mg/mL, η_{rel} ~ 2) at different values of f (mass of mucin with respect to the total mass) and the viscosity of the mixed solutions was determined. Figures 2a and 2b show the typical outcome of microviscosimetry experiments, i.e. the percentage deviation of the viscosity of the mixed solutions from an additive line as a function of f (Equations 1 and 2). The experiments yielded examples of zero deviation (no interaction), increase in viscosity (positive synergy) and decrease in viscosity (negative synergy or antagonism). For example, mixtures of mucin with the neutral and highly-branched polysaccharide dextran (Dex) in water (pH 4.5) showed no appreciable deviation from the additive line, indicating that there was no interaction (Figure 2a). In contrast, mixtures of mucin and the negatively-charged, sulfated form of dextran showed a substantial deviation from the additive line (Figure 2a), although the nature of the interaction was dependent on the Mw. Mixtures of mucin and low-Mw DexS40 showed greater viscosity at all f ratios tested up to ~14% at the point of maximum interaction (f = 0.4), whereas mixtures of mucin and high-Mw DexS500 showed a sharp reduction in viscosity (to a minimum value ~40% lower than the viscosity of the two stock solutions) at f = 0.9. Similar results were observed for alginate (Figure 2b), where the low-Mw polymer (Alg4) induced a slight but significant increase in viscosity (up to ~5%) throughout the entire range of f values, whereas its high-Mw counterpart (Alg400) showed negative synergy with a maximum at f = 0.9 (i.e. an excess of mucin). In neither system was there any evidence of turbidity or phase separation upon standing.

When two different macromolecular species (e.g. polysaccharide and protein) are mixed in solution, either attractive or repulsive interactions can take place.[34] Attractive interactions can result in the formation of a complex that either remains in solution or precipitates. Repulsive interactions can lead to phase separation or co-solubility.[34] In the case of associative interactions, the bulk viscosity of dilute mixed solutions is expected to decline because there is an overall reduction in the hydrodynamic volume of the macromolecules when they are combined, as observed in dilute mixed solutions of mucin and chitosan.[8,16] However, in other cases, cooperative intrapolymer and interpolymer interactions can increase the viscosity and even induce gelation, as observed in alginate–mucin,[9] xanthan–galactomannan[24] and alginate–pectin systems.[10] Repulsive interactions are expected to maintain the viscosity of mixed solutions at values similar to the individual stocks. However, if the conformation of one of the molecules changes because it is excluded to a segregated phase, the viscosity of the mixture can also deviate from the expected additive line.

Under our dilute experimental conditions, polymer exclusion effects were assumed to be negligible[24] and it is reasonable to postulate that the observed changes in viscosity reflected heterotypic interactions.

Dextran is a neutral polymer that behaves in aqueous solutions as a random flexible coil.[35] It is also a compact molecule due to the presence of branching[36] and 1→6 glycosidic linkages. These properties explain the absence of interactions with mucin, reflecting its inability of dextran to undergo significant contraction in response to ionic strength variation (Fig. 1). This is consistent with previous experiments studying the adsorption of dextran on a mucin-modified gold-coated quartz crystal microbalance.[37] The interaction between polyions and water-soluble non-ionic polysaccharides may depend on a Mw threshold below which interpolymer complexes do not form, as observed for PAA and hydroxyethylcellulose.[38] It is unclear whether higher-Mw dextran interacts with mucin, but the mucoadhesive properties of dextran can be increased by introducing functional groups that increase its hydrophobicity (e.g. methyl groups)[37] or polyelectrolyte properties (e.g. sulfate groups).

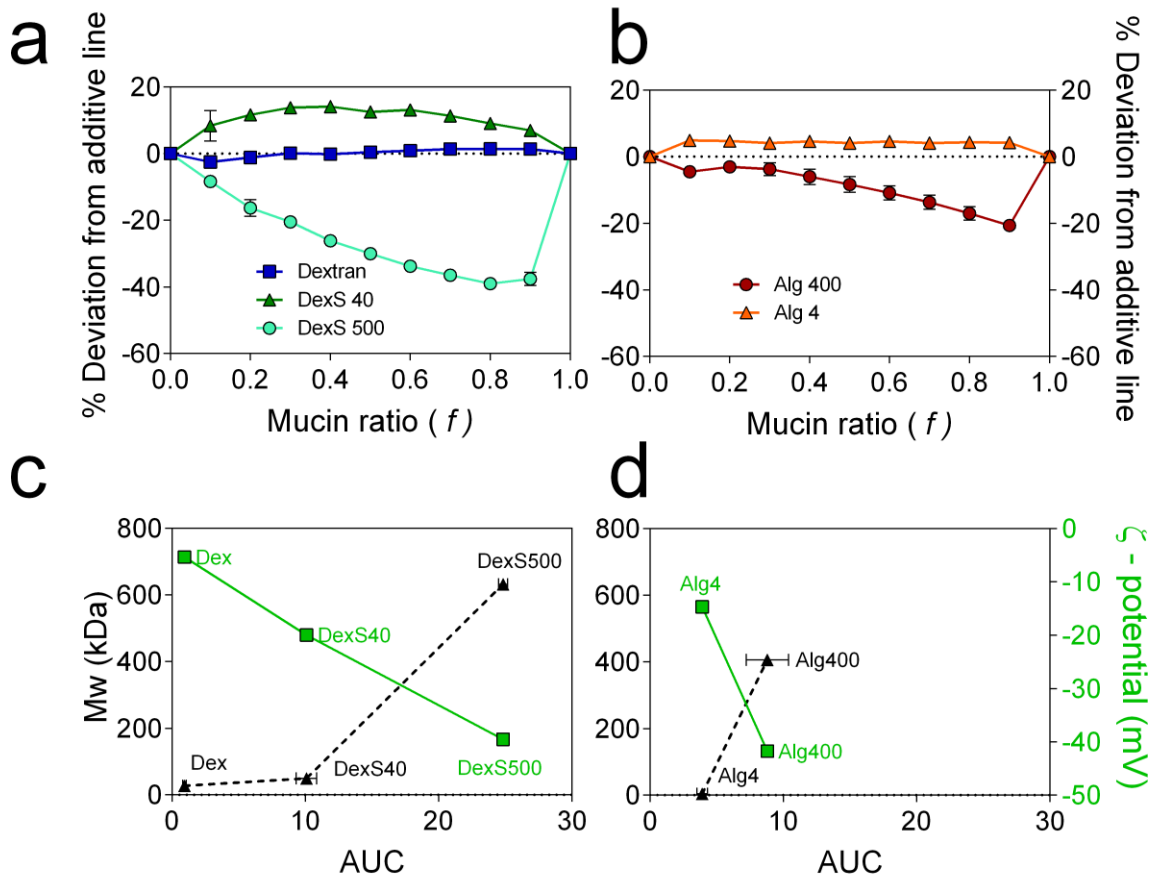

Figure 2. Percentage deviation of the η_{rel} of a) mucin–dextran and b) mucin–alginate mixtures in water (37°C, pH 4.5) with respect to the additive line of non-interaction, based on

microviscosimetry data. Panels c and d show the dependency of the AUC (integrated area under the curve described by the points at the different f values and the additive "zero" baseline) on the Mw (dashed line) and charge expressed as ζ-potential for dextrans and alginates. Lines indicate the observed trend.

Although several studies have addressed the mucoadhesion properties of dextran sulfate, the main derivative of dextran, little is known about the underlying mechanisms. We have confirmed that dextran sulfate interacts with mucin, as revealed by the changes in viscosity, but the Mw of the polysaccharide plays a prominent role in this interaction.

Next we calculated the integrated area under the curve (AUC) described by the points at the different f values and the additive "zero" baseline for each polysaccharide–mucin system, in order to quantify each interaction. DexS500 had an absolute AUC value greater than that of DexS40 (although the direction of synergy was different in each case), which in turn was slightly greater than that of neutral dextran. Figure 2c shows that the ability of dextran sulfate to interact with mucin increases with Mw and with a more negative ζ-potential (Eq. 3) and a similar trend is shown for alginates in Figure 2d. These results support previous experiments based on dynamic light scattering (DLS) and isothermal titration calorimetry showing that the interaction between protein and alginate increases with increasing Mw.[39]

Mucin can be defined as a "gel of complexity" based on the presence of (i) numerous O-linked glycans on threonine and serine hydroxyl groups, (ii) strong proton acceptor and donor groups in the heavily-glycosylated region, and (iii) a cysteine-rich naked region, offering diverse opportunities for multiple forces to combine during protein–polysaccharide interactions. There is a pH gradient in the mucus layer of the stomach,[40] so mucin can undergo conformational transitions that favor either mucin–mucin or polymer–mucin interactions under different conditions. For example, the extended conformation is maintained by repulsive electrostatic interactions between negatively-charged sialic and carboxylic acid residues at neutral pH, but under strongly acidic conditions (pH < 2) these residues are protonated and the tertiary structure of mucin changes so that hydrophobic regions are exposed, mucin–mucin interactions are favored and a sol to gel transition occurs.[41,42]

Commercial mucin may not provide an accurate model for natural mucous membranes because they have distinct rheological properties[43] but commercial mucin yields reproducible results because there is little batch-to-batch variability.[16,44] The soluble fraction of partially purified porcine gastric mucin conserves the main structural properties of the molecule required for pH-dependent conformational changes and interactions with polysaccharides (Fig. 3a) as previously described for both commercial and non-commercial preparations.[44,45] Mucin displays a negative ζ-potential at

neutral pH which declines as the environment becomes more acidic, and the size of the molecule increases until it reaches a peak at the neutrality point (pH ~2) as shown by the longer relaxation time in Figure 3b. At lower pH values there is a decrease in size, attributed to the contraction of the interchain complexes stabilized by protonated residues.[45] However, we did not observe an inversion of the ζ-potential to positive values.

Most of the charged polysaccharides we tested showed a greater or lesser tendency to interact with mucin. Although the net surface charge of mucin in the pH range 3–6 is negative (hence our choice of pH 4.5 for testing), the neutral/charged amino acids along the mucin backbone are not uniformly distributed.[5] The interaction between polyanions and mucin at pH 4.5 may be predominantly electrostatic, involving patches of positive charge (arginine, histidine and lysine) in the mucin protein backbone, as previously discussed in the case of alginate–mucin interaction[46]. The AUC results for all the polysaccharides we tested are summarized for tests in water (Fig. 4a) and in 0.1 M NaCl (Figure 4b). The highest values were observed when the interaction was measured in water. The presence of 0.1 M NaCl tended to suppress most of the mucin–polysaccharide interactions, although chitosan–mucin interactions were preserved under these conditions, with substantial AUC values that varied according to the Mw and degree of acetylation.[8] The ability of NaCl to attenuate the putative interaction between polyanions and mucin indicates that ionic interactions play a key role.

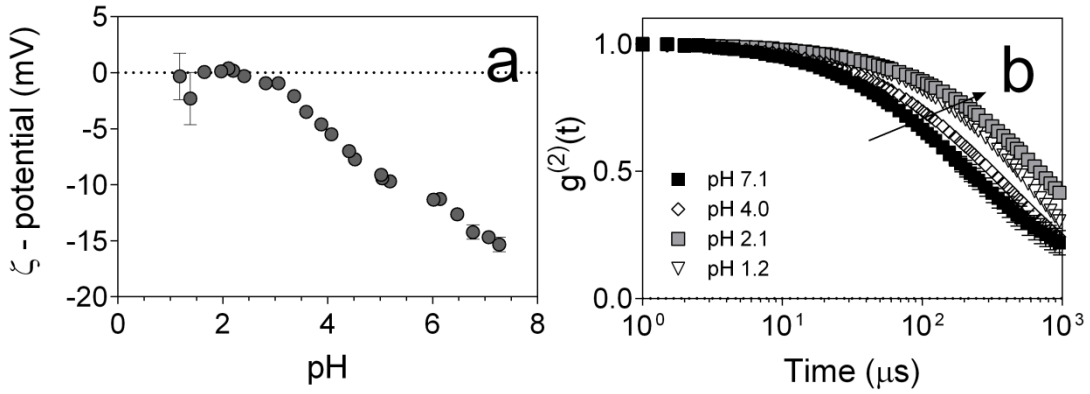

Figure 3. a) Variation in the ζ-potential of the soluble fraction of Sigma-Aldrich partially-purified porcine gastric mucin (5 mg/ml) during pH titration, determined using an MPT-2 autotitrator connected to the M3-PALS/DLS-NIBS Malvern Zetasizer Nano ZS (25°C).

Previous studies have shown that mucoadhesion in the urinary bladder mucosa is reduced in the presence of sodium, calcium and magnesium ions, with calcium ions playing the predominant

role.[47,48] In the case of mucin, calcium ions mediate a highly-cooperative transition process which promotes the agglomeration of mucin during mucin granule biogenesis.[49]

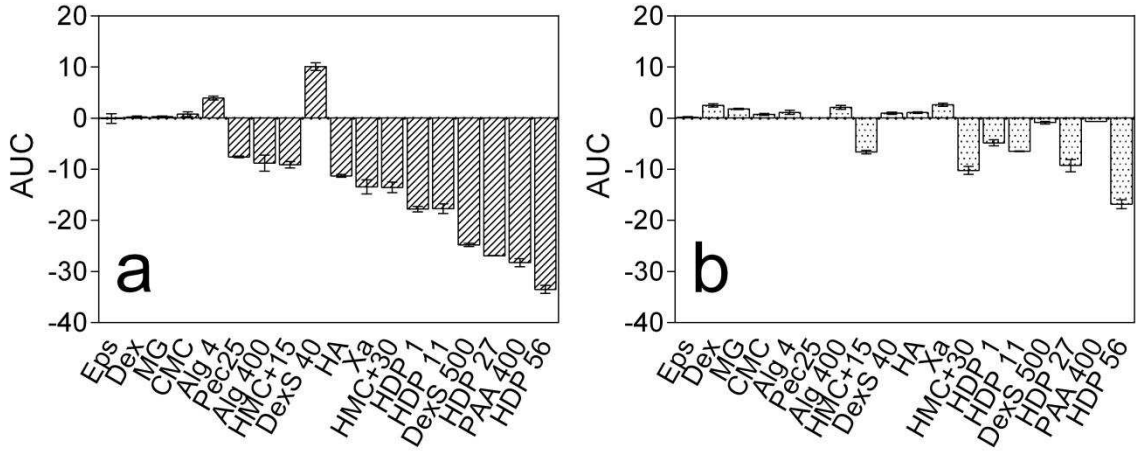

Figure 4. The interaction between mucin and polysaccharides in a) water and b) 0.1 M NaCl, both at pH 4.5. Each interaction is expressed as the area under the curve (AUC) representing the percentage deviation in the viscosity values of mixed solutions with respect to the additive line (n = 2; mean ± minimum and maximum values).

In chitosan–mucin systems, the components carry oppositely charged groups and electrostatic forces are therefore prevalent, but other forces are also involved[44] which can be attributed to the particular structural features of chitosan.[8] Only a few systems showed no evidence of interaction (EPS, dextran, MQ and CMC). A loss of viscosity (negative AUC values) was observed for high-Mw chitosan, PAA and DexS500, which also showed AUC values of the greatest magnitude.

Polysaccharide charge is a fundamental component of interactions with mucin

The electrophoretic mobility (μ_e) and hence the ζ-potential of a polyion is generally a function of its net surface electrical charge and is inversely proportional to the friction coefficient.[50] It is therefore expected to be a function of the shape and size of the macromolecule, the nature and pH of the solvent, and the electrolyte. The dependence of μ_e on charge density has been explained in the context of Manning's ion condensation theory.[51] In the case of chitosan, there is proportionality between μ_e and the charge density reflecting its weak charge and the absence of counter-ion condensation.[52] Under the conditions we used to characterize the μ_e of our polysaccharides (concentration at η_{rel} ~2, pH 4.5 and 37°C) the net charge influenced the interaction between polysaccharides and mucin. Indeed, the neutral μ_e of dextran, EPS and MQ correlated with their

poor interactions with mucin, whereas highly-charged polysaccharides with high μ_e values interacted with mucin strongly. However, there was no consistent correlation between the increase in μ_e and AUC. Indeed, Pec25 had the highest μ_e but the lowest AUC among the polyanions we tested. In contrast, the μ_e of CMC was half that of Pec25 and they have different AUC values, yet both interact only weakly with mucin.

EPS is an exopolysaccharide from the lactic acid bacterium Streptococcus thermophilus 1190 which helps to prevent gastritis by protecting the stomach from inflammation[53] and preventing the adhesion of Helicobacter pylori to the mucus layer.[21] The analysis of its mucoadhesive capacity by microviscosimetry contradicted immunofluorescence data in which FITC-labeled EPS1190 was applied to sections of human gastric mucosa, reflecting differences between the soluble fraction of porcine gastric mucin used in vitro and the native mucosal surface.[21] However, the absence of uronic acid in EPS1190 as determined by monosaccharide composition analysis[21] and confirmed by the neutral μ_e, suggests that (like dextran) it is not an ideal mucoadhesive candidate.

Mesquite gum (MQ) is a high-Mw type II arabinogalactan, which is slightly acidic (due to the presence of a small number of glucuronate residues), highly-branched, heterogeneous and polydisperse.[23] Dextran, MQ and EPS not only display a common lack of interaction with mucin, but they also possess an almost neutral charge, a compact chain and a limited ability to contract in response to environmental changes. This agrees with the result of an ex vivo assay on colonic tissue which revealed that FITC-labeled dextran, arabinogalactan and citrus pectin do not interact with mucosal tissue.[54] Neutral non-interacting polymers can thus be used to coat the surface of nanoparticles to increase their mucopenetrating properties (e.g PEG).[55]

Higher chain flexibility enhances interactions with mucin

Although the electrical charge density determines whether or not a polysaccharide interacts with mucin, the unique properties of each mucin–polysaccharide system, as shown by the AUC and the optimal f ratio, suggest other polysaccharide characteristics such as the chain size, chain flexibility, the nature of the charged groups (e.g. SO_3^-, COO^- or NH_3^+) and even the presence of high-affinity structural patterns “written” in the polysaccharide primary structure, may also play a significant role. The degree of contraction, here expressed as the $[\eta]_{H20}/[\eta]_{NaCl}$ ratio, accurately reflects the behavior of charged macromolecules in solution based on their polyelectrolyte characteristics. Such conformational molecular adaptation is necessary for a polysaccharide to be mucoadhesive. Chain flexibility has been suggested to maximize the formation of heterotypic contact points between the polymer and the corresponding part of the mucin molecule, thus promoting interpenetration and

entanglement.[56] We found that the strength of the interaction between polyanions and mucin (represented by the AUC) depends on the degree of contraction. Figure 5a shows the curve of the $[\eta]_{H_2O}/[\eta]_{NaCl}$ ratio for polyanionic polymers mixed with mucin in water (pH 4.5). The trace shows a monotonic dependence on the absolute AUC (regardless of the direction of synergy). In general, the AUC increases with the degree of contraction, thus the higher degree of contraction shown by Alg400 (4.65) compared to Alg4 (1.19) and by DexS500 (10.89) compared to DexS40 (3.79) might explain the higher absolute AUC values for Alg400 and DexS500. At the bottom-left corner of the best non-linear fit curve, Alg4, Pec25 and CMC had the lowest AUC values.

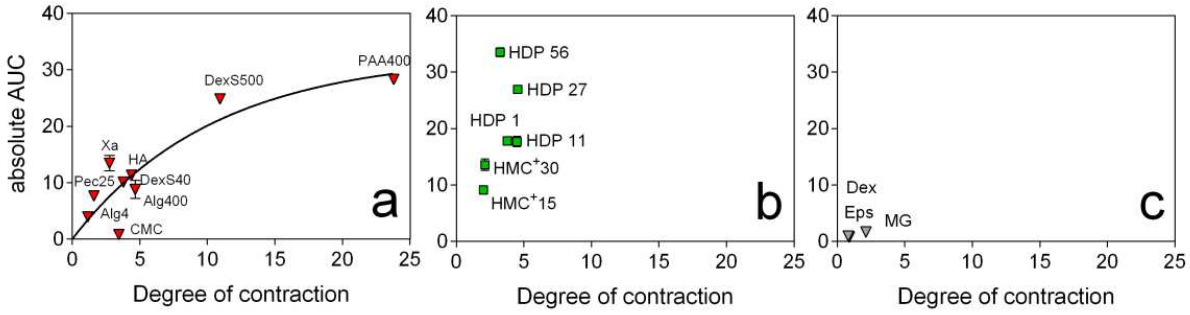

Figure 5. Correlation between mucin–polysaccharide interactions expressed as the absolute AUC (regardless of the direction of synergy) and degree of contraction for a) polyanions, b) polycations, and c) neutral polysaccharides.

CMC did not have the lowest degree of contraction (3.79) but nevertheless it did not interact with mucin under our conditions. Previous studies based on rheological synergism have shown that Na-CMC is mucoadhesive.[14,57] However, our data support studies in which CMC showed only transient adhesion to a mucosal surface,[58] the least degree of rheological synergism in mucin gels[59] and the weakest force of detachment from mucus-covered slides in saline solution, artificial gastric juice and intestinal fluid.[12] This discrepancy again reflects the diverse methods, conditions and approaches used to study such interactions, differing in sensitivity, the detection process, the state of mucin (gel or dilute solution) and the concentration and state of the dissolved polysaccharide.

In the midrange of the AUC vs degree of contraction curve, Xa, Ha, DexS40 and Alg400 shared similar values whereas DexS500 showed the highest degree of contraction and the strongest interaction with mucin among the natural polyions. Although the more flexible, negatively-charged polysaccharides always interacted more strongly with mucin than the low-Mw and less flexible molecules, no further benefit was achieved at higher degrees of contraction. PAA displayed a degree of contraction double that of DexS500 but the AUC was only 11% larger.

Neutral polysaccharides lacked the capacity to interact with mucin (Fig, 5c). In turn, positively-charged chitosan molecules did not conform to the general pattern observed for polyanions (Fig. 5b). These results confirm that mucoadhesion is based on more complex mechanisms than chain adaptation and electrostatic interactions. Our earlier investigation of chitosan mucoadhesion revealed that the capacity for interaction depends on the structural features of the polysaccharide, specifically the Mw and degree of acetylation.[8]

Although chain conformation, polymer adaptation and the various underlying interactions combine to produce the viscosity response observed in polysaccharide–mucin mixtures, the precise molecular mechanisms remain unclear. Mucin and the low-Mw Alg4 showed a slight positive synergy, perhaps reflecting the formation of an extended network as reported in galactomannan–xanthan mixed systems,[24] whereas mucin and high-Mw Alg400 showed negative synergy, perhaps reflecting a heterotypic interaction based on conformational adaptation. However, the magnitude of the synergistic increase in η_{rel} when mucin is mixed with Alg4 or DexS40 was much lower than that of dilute galactomannan–xanthan systems. Our data are consistent with the notion that low-Mw alginate molecules (and possibly other low-Mw polyanions) are too small to experience a significant coil contraction and hence are less able to interact with the whole structure of mucin in the manner of larger chains. To gain insight into this phenomenon we investigated the alginate–mucin system in greater detail using scattering and fluorescence spectroscopy.

DLS-NIBS and synchrotron SAXS analysis confirm the molecular interaction between mucin and alginates

DLS-NIBS measurements in mixed alginate–mucin systems revealed that mucin at pH 4.5 exists as highly polydisperse colloidal species (PDI > 0.5) whose size changes according to the pH (Figure 3b). The presence of Alg4 did not appear to induce any consistent variation in the bulk size of mucin at any of the f ratios tested, as shown by the negligible impact on the shape of the relaxation time curves and relaxation times (Figure 6a). In contrast, the correlation function of mucin in the presence of Alg400 at ratios < 0.4 shifts to a longer relaxation time, suggesting the formation of larger species (Figure 6b). However, at higher f ratios, the curves resemble the profiles of mucin alone, characterized by species of lower dimensions.

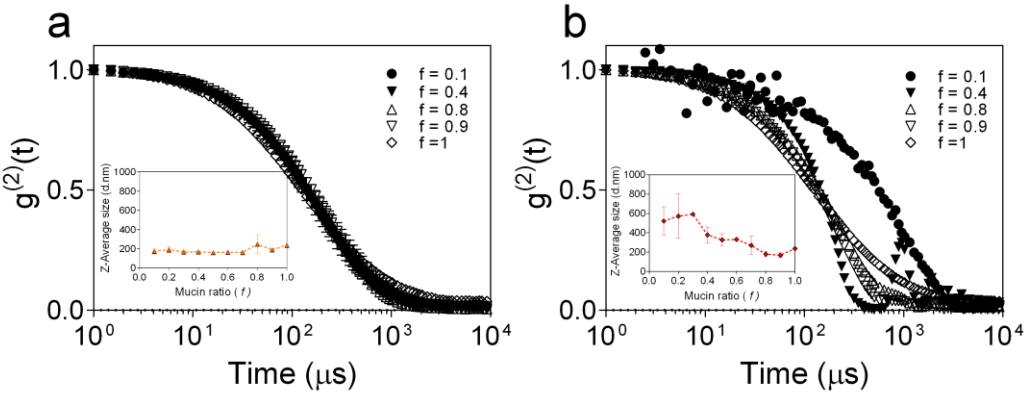

Figure 6. Normalized correlation functions versus time for a) mucin–Alg4 and b) mucin–Alg400 mixtures analyzed at 173° by DLS-NIBS in a Malvern Zetasizer Nano ZS (in water at 37°C). Insets showed the extrapolated Z-Avarage size values.

A reduction in the hydrodynamic volume of the species in solution (represented by a decline in the viscosity of Alg400–mucin at f = 0.9) was accompanied by a proportional reduction in the size of Alg400–mucin as reported by DLS-NIBS. Previous analysis of alginate–mucin systems by DLS and viscosimetry[11] revealed that the hydrodynamic radii of species formed in the mixed solutions were smaller than those of the individual components. This is consistent with our results showing that the overall dimensions of mucin change in the presence of high-MwAlg400.

The detailed macromolecular structure of mucin has previously been investigated using high-resolution scattering techniques, such as synchrotron SAXS,[60,61,62] SANS,[61,26,63], static light scattering (SLS) and DLS[64] to compare the properties of mucin samples with different biological origins and preparation methods. The cylindrical model and the more recent double-globular comb model have therefore been used to account for the complex structure of mucin.[60,63,64] Aqueous solutions of bovine submaxillary mucin studied by SAXS displayed an expanded chain conformation at low concentrations (1.4–3.6 mg/mL) but a Gaussian chain conformation at higher concentrations (> 7 mg/mL).[62] More recent studies have addressed the impact of concentration on the structure of mucin and the existence of a coil overlap concentration (c*), along with other parameters as measured by a combination of SLS, DLS and rheology, concluding that c* = 1.54 mg/mL in water.[63] Our SAXS data (Figure 7a) revealed that mucin displays an intensity scattering curve (i.e. I(q) vs q) characterized by a one-fractal dimension with a value of the Porod exponent (d_f = –1.6) at a concentration of 3.0 mg/mL, which supports the results of previous studies.[60,61] This fractal regime has been observed in a concentration range of 1.4–20 mg/mL.[61,62] At lower concentrations (0.3 mg/mL), the scattering curve (Figure 7a) allowed us to fit the Guinier function

(log I(q) vs. q^2, inset in Figure 7a) and to calculate a radius of gyration (R_g) of 18 ± 3 nm. This is somewhat lower than the R_g values reported for Sigma and Orthana commercial porcine stomach mucin and for purified mucin samples, i.e. 23–42 nm at a pH value above the sol to gel transition point and under low salt conditions.[61,60,63]

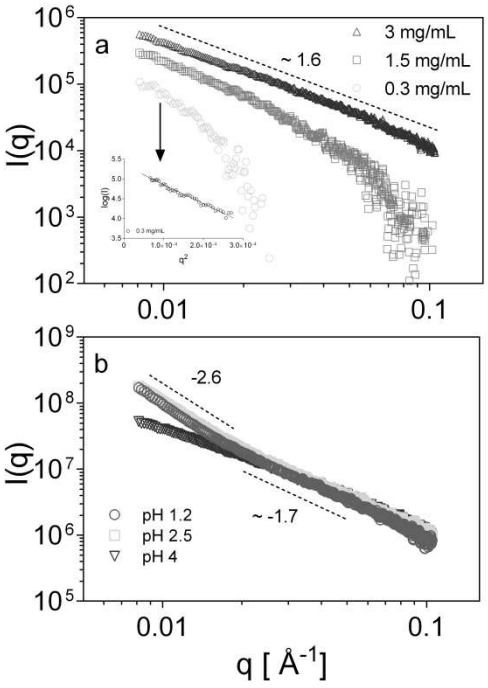

Figure 7. Synchrotron SAXS scattering profiles of the soluble fraction of porcine stomach mucin (type III) at a) 3 mg/mL (triangles), 1.4 mg/mL (squares) and 0.5 mg/mL (circles), and b) different pH values. The inset in panel (a) shows the Guinier region of the more diluted sample extracted at q values such that $q \times R_g < 1$.

The SAXS data suggest that our mucin preparation did not contain aggregates or highly-entangled insoluble fractions as indicated in previous studies[61] which would have increased the value of R_g. A second d_f exponent greater than –1.6 appeared in the scattering curves of 3.0 mg/mL mucin in the low-q range at pH 1.2 and 2.5 (Figure 7b). This agrees with similar pH-driven transitions reported previously.[61] Although commercial mucin preparations may not undergo a sol-gel transition due to the use of chaotropic salts and reducing agents during extraction and purification[61] the observed change in the slope at low pH values is consistent with the existence of a conformational transition in our mucin sample. Further studies will confirm the validity of this hypothesis using other techniques such as circular dichroism spectroscopy.

SAXS was used to gain insight into the interactions between mucin and alginate and the potential underlying mechanisms. Figures 8a-c show the scattering curves for mixtures of mucin and low-Mw Alg4 at mucin concentrations of 3.0, 1.5 and 0.3 mg/mL, whereas Figures 8d-f show the corresponding curves for mixtures of mucin and high-Mw Alg400 at the same mucin concentrations. In the case of Alg4, sufficient alginate was added to span the range f = 0.1–0.93, whereas the range was narrower in the case of Alg400 (f = 0.8–0.99). These f ratios were selected based on our microviscosimetry data (Figure 2). In the Alg4 mixtures, slight positive synergy was observed throughout the range of f values whereas in the Alg400 mixtures the greatest reduction in viscosity was observed at higher f ratios (cf. Figure 2). The scattering curves in Figures 8a and 8d, corresponding to a large excess of mucin over alginate (f = 0.93 for Alg4 and f = 0.99 for Alg400), show that the slopes of the linear fit calculated throughout the q range remain close to –1.6 and the curves are almost identical to the mucin curve without alginate. These data confirm that the fractal regime in the mucin–alginate mixtures persists from the mucin solution without alginate, with mucin at the same concentration (see Figure 7a). This may reflect the fact that mucin has a more contracted conformation at $c > c^*$ and it is less sensitive to structural changes in the presence of minute amounts of alginate regardless of the Mw. However, at lower mucin concentrations ($c \sim c^*$) the scattering profile becomes reminiscent of mucin alone at a higher concentration (Figures 8b and 8e). Indeed, this effect is even more pronounced in the mixed systems with the lowest concentration of mucin (0.3 mg/mL) in which $c < c^*$ (Figures 8c and 8f). The most remarkable difference between the two polymers is observed in the high-q range. Here, the presence of low-Mw Alg4 (Figure 8c) results in a mucin scattering profile which, in the low-q range, resembles that of mucin alone at a low concentration, whereas in the high-q range the curve is similar to that of mucin alone at higher concentration. Between these distinct regions is a plateau zone with a slope of approximately –0.3. The effect is less pronounced for Alg400, where the high-q region resembles mucin alone at a low concentration. Table 2 summarizes the corresponding analysis of the Porod exponents of mucin and mucin–alginate mixtures at the three tested concentrations.

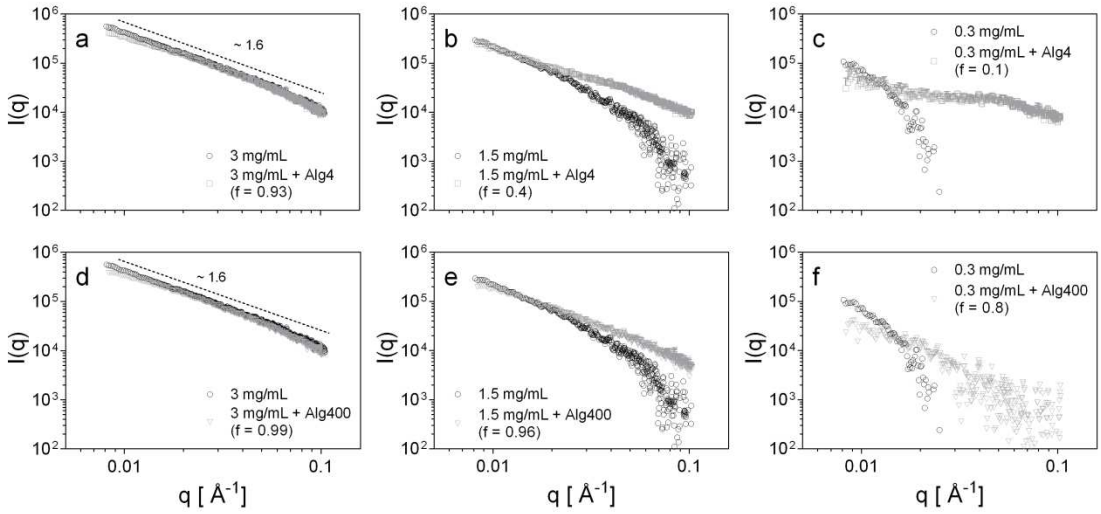

Figure 8. Synchrotron SAXS scattering intensity profiles in water at pH 4.5 and 25°C. a) Mucin and mucin–Alg4 (3 mg/mL mucin). b) Mucin and mucin–Alg4 (1.5 mg/mL mucin). c) Mucin and mucin–Alg4 (0.3 mg/mL mucin). d) Mucin and mucin–Alg400 (3 mg/mL mucin). e) Mucin and mucin–Alg400 (1.5 mg/mL mucin). f) Mucin and mucin–Alg400 (0.3 mg/mL mucin).

Table 2. Values of the power law-fit exponents ($I(q) \sim q^{slope}$) of synchrotron SAXS data of mucin at different concentrations in the presence and absence of alginate throughout the whole q-range or only in the high-q range (0.052–0.1 $Å^{-1}$).

Mucin (mg/mL)	Alginate	High-q		All range	
		Slope	R^2	Slope	R^2
3	-	-1.893	0.972	-1.583	0.992
3	Alg400	-1.958	0.978	-1.586	0.989
3	Alg4	-1.944	0.976	-1.559	0.989
1.5	-	*	*	-2.717	0.875
1.5	Alg400	-1.958	0.913	-1.610	0.981
1.5	Alg4	-1.873	0.970	-1.312	0.970
0.3	-	*	*	*	*
0.3	Alg400	*	*	-2.113	0.732
0.3	Alg4	-1.298	0.870	-0.641	0.819

*Power law-fit not possible

Our synchrotron SAXS data for mucin–alginate mixtures in solution (rather than gels, as in previous studies) confirmed that low-Mw Alg4 interacts with mucin, presumably involving positively-charged patches of the protein globules (i.e. von Willebrand-like domains) without affecting the overall expanded conformational state of mucin. Such interactions therefore do not influence the bulk properties of the solution such as viscosity and hydrodynamic size (Figure 6). This interpretation was previously used to explain the ability of alginate oligomers (Mw ~2–4 kDa, DP ~10–19) to competitively inhibit the interaction between high-Mw alginate and mucin, thus preventing the formation of a gel by occupying available positively-charged sites[46] The formation of more compact alginate-mucin mixed species, whose overall dimensions do not change, may account for these results and the lack of size variation observed by DLS-NIBS.

The mucin–alginate interaction under our experimental conditions was confirmed by fluorescence spectroscopy (Fig. 9). The fluorescence emission intensity of mucin at λ_{ex} = 339 nm declined following the addition of small aliquots of both Alg4 and Alg400 (Fig. 9a and 9b, respectively), as previously observed for the interaction between mucin and oxymetazoline hydrochloride, a decongestant drug[65] and in our own studies of mucin-chitosan interactions.[8]

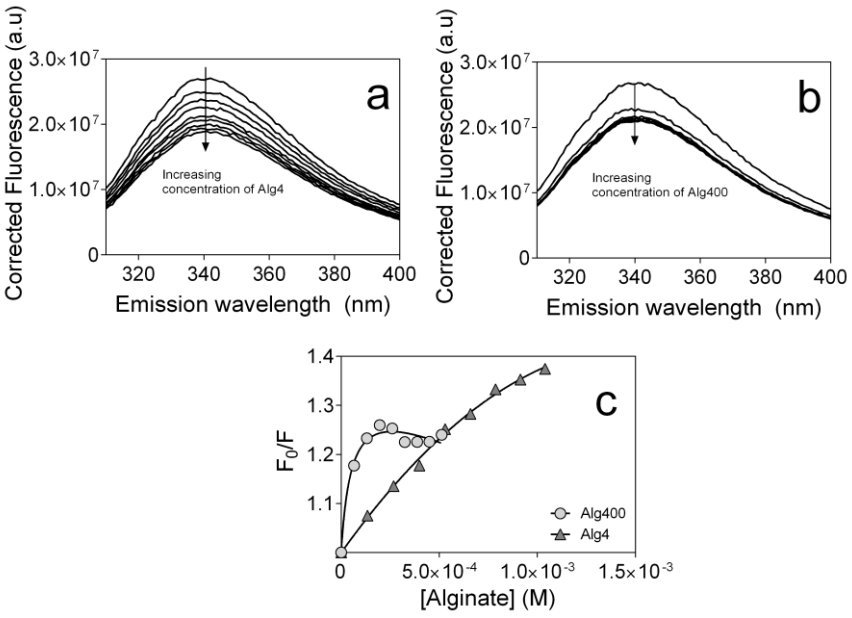

Figure 9. The fluorescence quenching spectra of mucin (0.5 mg/mL) at 25°C in acetate buffer (pH 4.5) following titration with a) Alg4 (0.13, 0.27, 0.40, 0.53, 0.66, 0.79, 0.91 and 1.04 µM) and b) Alg400 (0.07, 0.13, 0.20, 0.26, 0.32, 0.39, 0.45 and 0.51 µM); c) Variation in the relative fluorescence intensity (λ_{ex} = 295 nm and λ_{em} = 338 nm) as a function of the alginate concentration.

The fluorescence quenching data provides unequivocal evidence that mucin interacts with both alginates. The corresponding Stern-Volmer curves (F_0/F vs alginate concentration) show that both alginate–mucin systems are characterized by downward curvature (Fig. 9c), which usually represents quenching on a heterogeneous protein.[66] However, there are important differences between the curves reflecting the different Mw-dependent binding mechanisms of the two alginates. The curve for high-Mw Alg400 is stiffer and reaches a plateau at an alginate concentration of 0.20 µM, whereas the curve for low-Mw Alg4 is monotonic and the quenching effect persists up to at least 1.04 µM, the highest concentration tested. This suggests that Alg400 has a higher capacity than Alg4 for the formation of complexes with mucin, but more of the tryptophan groups in the protein fraction becomes more exposed with Alg4 resulting in more pronounced fluorescence quenching.[67] This is consistent with the interpretation of our SAXS data (Figures 8c and 8f) showing that Alg4 can affect the structure of mucin at smaller length scales, probed at the high-q end of the SAXS scattering curves.

Our microviscosimetry, scattering and spectroscopy data converge on a model of interaction between mucin and anionic polysaccharides as a function of Mw, charge and degree of contraction (Fig. 10). Mucin can be described in terms of double-globular protein regions connected by highly glycosylated linkers. The carbohydrate residues contain functional groups (e.g. carboxylic and sialic acids) that are negatively charged at pH > 2.5 thus maintaining the expanded conformation of mucin by repulsive interaction, particularly in the absence of salt and at concentrations $c < c^*$. Although the overall net charge of mucin is negative, positively-charged patches are likely to exist in the non-glycosylated globular regions containing histidine, arginine and lysine residues. These represent potential sites for interaction with negatively-charged polysaccharides. Low-Mw and stiff polyanions (Fig. 10a) are likely to interact preferentially with these globular regions without influencing the preferred conformation of mucin, thus having a negligible impact on bulk properties such as size and viscosity but evident in the high-q range of the SAXS scattering curves. In such case, the polyanion is small enough to penetrate the globular structure of mucin, inducing the rearrangement of the protein and exposing aromatic residues as evidenced by the pronounced fluorescence quenching. This rearrangement may eventually favor cross-linking of mucin which is consistent with the observed slight increase in viscosity. This hypothesis is in consonance with the cross-linking mechanism proposed to explain the gelation of mucin in the presence of polyphenols.[26] In contrast, high-Mw polyanions are more flexible and are likely to bridge distant sites thus influencing the conformation of mucin and favoring a reduction in the overall hydrodynamic volume (Fig.10b). This reduces the availability of interacting sites for additional polymer molecules and also occupies multiple sites simultaneously, saturating the available sites

more quickly than low-Mw polyanions and thus preventing fluorescence quenching at the early stages of titration. Such phenomena reduce the viscosity of the mixture especially at f ratios representing excess mucin. Although Mw is thought to play an important role in such interactions, chain flexibility determines the ability of high-Mw polysaccharides to induce the contraction of mucin.

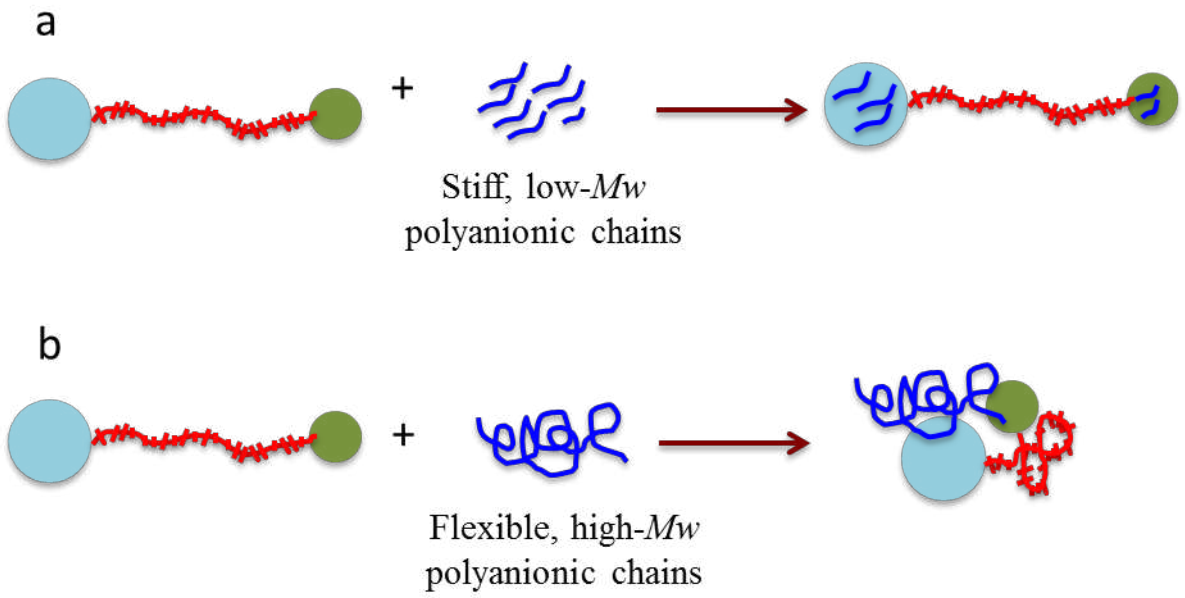

Figure 10. Model for the interaction between alginate and the double-globular comb structure of mucin as a function of alginate Mw and chain flexibility.

Conclusions

The physicochemical properties of polysaccharides are diverse and their interactions with mucin must be investigated on a case-by-case basis using standardized components and methods to avoid experimental variations. We have carried out a systematic analysis of the mucoadhesive properties of polysaccharides using defined experimental conditions (i.e. initial viscosity of the polysaccharide and mucin solutions), sensitive equipment, and a combination of data from different molecular levels, i.e. macroscopic data from microviscosimetry experiments and nanoscopic data from scattering experiments. This allowed us to characterize mucin–polysaccharide interactions in detail according to the molecular weight, charge and degree of contraction of the polysaccharide chain. We found that highly-charged polymers with a high degree of contraction interacted more strongly with mucin as shown by the substantial reduction in the viscosity of the mixture compared to the stock solutions. This approach also distinguished among different degrees of interaction with the

fine structure of mucin, allowing us to focus on selected low-Mw and high-Mw alginates for more detailed analysis. Different degrees of interference with the fine structure of mucin indicated by opposite directions of synergy in the microviscosimetry experiments were confirmed by scattering techniques and spectroscopy. The proposed model is an oversimplification of the complex hierarchical supra-molecular organization of mucin and its interactions with other polyanions. However it offers a general explanation to account for the interactions of mucin and polyanions of varying characteristics in solution. The utilization of other biophysical techniques such as quartz crystal microbalance (QCM), spectroscopy ellipsometry, colloidal probe reflection interference contrast microscopy, among other, will undoubtedly enable to expand the gained understanding in to far more complex systems of mucin surfaces in gel state. Finally, our results provide a rational approach for the selection of polysaccharides suitable for the development of mucoadhesive or mucopenetrating carriers for the delivery of drugs to mucosal surfaces in vivo.

Acknowledgements

We acknowledge financial support and a PhD fellowship to BM and JPF from the German Research Council DFG (Project GRK 1549, International Research Training Group 'Molecular and Cellular Glyco-Sciences') and a grant from the European Synchrotron Radiation Facility (CH 3386) to perform synchrotron SAXS studies in Grenoble. We thank Dr. Richard M. Twyman for critical reading of the manuscript.

Supporting information

A table is provided summarizing the main characteristics of the polymers used in this investigation, including the primary structure, functional groups and biological properties. This material is available free of charge at http://pubs.acs.org.

References

1. Liu, Z. H.; Jiao, Y. P.; Wang, Y. F.; Zhou, C. R.; Zhang, Z. Y., Polysaccharides-based nanoparticles as drug delivery systems. Adv. Drug Delivery Rev. **2008,** 60, 1650-1662.

2. Park, K.; Robinson, J. R., Bioadhesive Polymers as Platforms for Oral-Controlled Drug Delivery - Method to Study Bioadhesion. Int J Pharm **1984,** 19, 107-127.

3. Sudhakar, Y.; Kuotsu, K.; Bandyopadhyay, A. K., Buccal bioadhesive drug delivery - A promising option for orally less efficient drugs. Journal of Controlled Release **2006,** 114, 15-40.

4. Suk, J. S.; Lai, S. K.; Boylan, N. J.; Dawson, M. R.; Boyle, M. P.; Hanes, J., Rapid transport of muco-inert nanoparticles in cystic fibrosis sputum treated with N-acetyl cysteine. Nanomedicine-Uk **2011,** 6, 365-375.

5. Lieleg, O.; Vladescu, I.; Ribbeck, K., Characterization of particle translocation through mucin hydrogels. Biophys J **2010,** 98, 1782-9.

6. Lai, S. K.; Wang, Y. Y.; Hanes, J., Mucus-penetrating nanoparticles for drug and gene delivery to mucosal tissues. Adv Drug Deliver Rev **2009,** 61, 158-171.

7. Sosnik, A.; das Neves, J.; Sarmento, B., Mucoadhesive polymers in the design of nano-drug delivery systems for administration by non-parenteral routes: A review. Progress in Polymer Science **2014**.

8. Menchicchi, B.; Fuenzalida, J. P.; Bobbili, K. B.; Hensel, A.; Swamy, M. J.; Goycoolea, F. M., Structure of chitosan determines its interactions with mucin. Biomacromolecules **2014,** 15, 3550-8.

9. Taylor, C.; Pearson, J. P.; Draget, K. I.; Dettmar, P. W.; Smidsrød, O., Rheological characterisation of mixed gels of mucin and alginate. Carbohydrate Polymers **2005,** 59, 189-195.

10. Thirawong, N.; Kennedy, R. A.; Sriamornsak, P., Viscometric study of pectin–mucin interaction and its mucoadhesive bond strength. Carbohydrate Polymers **2008,** 71, 170-179.

11. Fuongfuchat, A.; Jamieson, A. M.; Blackwell, J.; Gerken, T. A., Rheological studies of the interaction of mucins with alginate and polyacrylate. Carbohyd Res **1996,** 284, 85-99.

12. Lehr, C.-M.; Bouwstra, J. A.; Schacht, E. H.; Junginger, H. E., In vitro evaluation of mucoadhesive properties of chitosan and some other natural polymers. International Journal of Pharmaceutics **1992,** 78, 43-48.

13. Hassan, E. E.; Gallo, J. M., A Simple Rheological Method for the Invitro Assessment of Mucin-Polymer Bioadhesive Bond Strength. Pharm Res **1990,** 7, 491-495.

14. Rossi, S.; Bonferoni, M. C.; Lippoli, G.; Bertoni, M.; Ferrari, F.; Caramella, C.; Conte, U., Influence of mucin type on polymer-mucin rheological interactions. Biomaterials **1995,** 16, 1073-9.

15. Ferrari, F.; Rossi, S.; Bonferoni, M. C.; Caramella, C.; Karlsen, J., Characterization of rheological and mucoadhesive properties of three grades of chitosan hydrochloride. Farmaco **1997,** 52, 493-7.

16. Rossi, S.; Ferrari, F.; Bonferoni, M. C.; Caramella, C., Characterization of chitosan hydrochloride-mucin interaction by means of viscosimetric and turbidimetric measurements. Eur J Pharm Sci **2000,** 10, 251-7.

17. Rossi, S.; Ferrari, F.; Bonferoni, M. C.; Caramella, C., Characterization of chitosan hydrochloride--mucin rheological interaction: influence of polymer concentration and polymer:mucin weight ratio. Eur J Pharm Sci **2001,** 12, 479-85.

18. Woertz, C.; Preis, M.; Breitkreutz, J.; Kleinebudde, P., Assessment of test methods evaluating mucoadhesive polymers and dosage forms: An overview. Eur J Pharm Biopharm **2013,** 85, 843-853.

19. Goycoolea, F. M.; Valle-Gallego, A.; Stefani, R.; Menchicchi, B.; David, L.; Rochas, C.; Santander-Ortega, M. J.; Alonso, M. J., Chitosan-based nanocapsules: physical characterization, stability in biological media and capsaicin encapsulation. Colloid Polym Sci **2012,** 290, 1423-1434.

20. Goycoolea, F. M.; Lollo, G.; Remunan-Lopez, C.; Quaglia, F.; Alonso, M. J., Chitosan-Alginate Blended Nanoparticles as Carriers for the Transmucosal Delivery of Macromolecules. Biomacromolecules **2009,** 10, 1736-1743.

21. Marcial, G.; Messing, J.; Menchicchi, B.; Goycoolea, F. M.; Faller, G.; Graciela, F. D.; Hensel, A., Effects of polysaccharide isolated from Streptococcus thermophilus CRL1190 on human gastric epithelial cells. Int J Biol Macromol **2013,** 62, 217-224.

22. Goycoolea, F. M.; Richardson, R. K.; Morris, E. R.; Gidley, M. J., Stoichiometry and Conformation of Xanthan in Synergistic Gelation with Locust Bean Gum or Konjac Glucomannan: Evidence for Heterotypic Binding. Macromolecules **1995,** 28, 8308-8320.

23. Lopez-Franco, Y. L.; de la Barca, A. M.; Valdez, M. A.; Peter, M. G.; Rinaudo, M.; Chambat, G.; Goycoolea, F. M., Structural characterization of mesquite (Prosopis velutina) gum and its fractions. Macromol Biosci **2008,** 8, 749-57.

24. Goycoolea, F. M.; Morris, E. R.; Gidley, M. J., Screening for synergistic interactions in dilute polysaccharide solutions. Carbohydr. Polym. **1995,** 28, 351-358.

25. Goycoolea, F. M.; Milas, M.; Rinaudo, M., Associative phenomena in galactomannan-deacetylated xanthan systems. Int J Biol Macromol **2001,** 29, 181-192.

26. Georgiades, P.; Pudney, P. D. A.; Rogers, S.; Thornton, D. J.; Waigh, T. A., Tea Derived Galloylated Polyphenols Cross-Link Purified Gastrointestinal Mucins. PLoS ONE **2014,** 9, e105302.

27. Georgiades, P.; Pudney, P. D. A.; Thornton, D. J.; Waigh, T. A., Particle tracking microrheology of purified gastrointestinal mucins. Biopolymers **2014,** 101, 366-377.

28. Rinaudo, M., Non-covalent interactions in polysaccharide systems. Macromol Biosci **2006,** 6, 590-610.

29. Morris, E. R.; Rees, D. A.; Welsh, E. J.; Dunfield, L. G.; Whittington, S. G., Relation between Primary Structure and Chain Flexibility of Random Coil Polysaccharides - Calculation and Experiment for a Range of Model Carrageenans. J Chem Soc Perk T 2 **1978**, 793-800.

30. Smidsrod, O.; Haug, A., Estimation of the relative stiffness of the molecular chain in polyelectrolytes from measurements of viscosity at different ionic strengths. Biopolymers **1971,** 10, 1213-27.

31. Kahovec, J. In Wormlike chain behaviour of some bacterial polysaccharides, Macromolecules 1992: Invited Lectures of the 34th IUPAC International Symposium on Macromolecules, 1993; VSP: 1993; pp 207-219.

32. Norton, I. T.; Goodall, D. M.; Frangou, S. A.; Morris, E. R.; Rees, D. A., Mechanism and dynamics of conformational ordering in xanthan polysaccharide. Journal of Molecular Biology **1984,** 175, 371-394.

33. López-Franco, Y. L.; Córdova-Moreno, R. E.; Goycoolea, F. M.; Valdez, M. A.; Juárez-Onofre, J.; Lizardi-Mendoza, J., Classification and physicochemical characterization of mesquite gum (Prosopis spp.). Food Hydrocolloids **2012,** 26, 159-166.

34. McClements, D. J., Non-covalent interactions between proteins and polysaccharides. Biotechnol Adv **2006,** 24, 621-625.

35. Carrasco, F.; Chornet, E.; Overend, R. P.; Costa, J., A generalized correlation for the viscosity of dextrans in aqueous solutions as a function of temperature, concentration, and molecular weight at low shear rates. Journal of Applied Polymer Science **1989,** 37, 2087-2098.

36. Senti, F. R.; Hellman, N. N.; Ludwig, N. H.; Babcock, G. E.; Tobin, R.; Glass, C. A.; Lamberts, B. L., Viscosity, Sedimentation, and Light-Scattering Properties of Fractions of an Acid-Hydrolyzed Dextran. J Polym Sci **1955,** 17, 527-546.

37. Chayed, S.; Winnik, F. M., In vitro evaluation of the mucoadhesive properties of polysaccharide-based nanoparticulate oral drug delivery systems. Eur J Pharm Biopharm **2007,** 65, 363-370.

38. Khutoryanskiy, V. V.; Mun, G. A.; Nurkeeva, Z. S.; Dubolazov, A. V., pH and salt effects on interpolymer complexation via hydrogen bonding in aqueous solutions. Polymer International **2004,** 53, 1382-1387.

39. Fuenzalida, J.; Nareddy, P.; Moreno-Villoslada, I.; Moerschbacher, B.; Swamy, M.; Goycoolea, F., Lysozyme–alginate nanocomplex: Effect of alginate composition. In Nanotechnology 2013: Bio Sensors, Instruments, Medical, Environment and Energy, NSTI: 2013; Vol. 3, pp 331 - 334.

40. Bahari, H. M. M.; Ross, I. N.; Turnberg, L. A., Demonstration of a Ph Gradient across the Mucus Layer on the Surface of Human Gastric-Mucosa Invitro. Gut **1982,** 23, 513-516.

41. Bansil, R.; Turner, B. S., Mucin structure, aggregation, physiological functions and biomedical applications. Curr Opin Colloid In **2006,** 11, 164-170.

42. Celli, J. P.; Turner, B. S.; Afdhal, N. H.; Ewoldt, R. H.; McKinley, G. H.; Bansil, R.; Erramilli, S., Rheology of gastric mucin exhibits a pH-dependent sol-gel transition. Biomacromolecules **2007,** 8, 1580-1586.

43. KocevarNared, J.; Kristl, J.; SmidKorbar, J., Comparative rheological investigation of crude gastric mucin and natural gastric mucus. Biomaterials **1997,** 18, 677-681.

44. Sogias, I. A.; Williams, A. C.; Khutoryanskiy, V. V., Why is chitosan mucoadhesive? Biomacromolecules **2008,** 9, 1837-1842.

45. Maleki, A.; Lafitte, G.; Kjoniksen, A. L.; Thuresson, K.; Nystrom, B., Effect of pH on the association behavior in aqueous solutions of pig gastric mucin. Carbohyd Res **2008,** 343, 328-340.

46. Nordgard, C. T.; Draget, K. I., Oligosaccharides As Modulators of Rheology in Complex Mucous Systems. Biomacromolecules **2011,** 12, 3084-3090.

47. Kos, M. K.; Bogataj, M.; Mrhar, A., Mucoadhesion on urinary bladder mucosa: the influence of sodium, calcium, and magnesium ions. Pharmazie **2010,** 65, 505-9.

48. Kerec, M.; Bogataj, M.; Mugerle, B.; Gasperlin, M.; Mrhar, A., Mucoadhesion on pig vesical mucosa: influence of polycarbophil/calcium interactions. Int J Pharm **2002,** 241, 135-143.

49. Verdugo, P., Goblet Cells Secretion and Mucogenesis. Annu Rev Physiol **1990,** 52, 157-176.

50. Xia, J. L.; Dubin, P. L.; Havel, H. A., Electrophoretic Light-Scattering Study of Counterion Condensation on Polylysine. Macromolecules **1993,** 26, 6335-6337.

51. Manning, G. S., Limiting laws and counterion condensation in polyelectrolyte solutions. 7. Electrophoretic mobility and conductance. The Journal of Physical Chemistry **1981,** 85, 1506-1515.

52. Strand, S. P.; Tømmeraas, K.; Vårum, K. M.; Østgaard, K., Electrophoretic Light Scattering Studies of Chitosans with Different Degrees of N-acetylation. Biomacromolecules **2001,** 2, 1310-1314.

53. Rodriguez, C.; Medici, M.; Mozzi, F.; de Valdez, G. F., Therapeutic effect of Streptococcus thermophilus CRL 1190-fermented milk on chronic gastritis. World J Gastroentero **2010,** 16, 1622-1630.

54. Schmidgall, J.; Hensel, A., Bioadhesive properties of polygalacturonides against colonic epithelial membranes. Int J Biol Macromol **2002,** 30, 217-225.

55. Wang, Y.-Y.; Lai, S. K.; Suk, J. S.; Pace, A.; Cone, R.; Hanes, J., Addressing the PEG Mucoadhesivity Paradox to Engineer Nanoparticles that "Slip" through the Human Mucus Barrier. Angewandte Chemie (International ed. in English) **2008,** 47, 9726-9729.

56. Smart, J. D., The basics and underlying mechanisms of mucoadhesion. Adv. Drug Delivery Rev. **2005,** 57, 1556-1568.

57. Smart, J. D.; Kellaway, I. W.; Worthington, H. E. C., An in-vitro investigation of mucosa-adhesive materials for use in controlled drug delivery. Journal of Pharmacy and Pharmacology **1984,** 36, 295-299.

58. Alireza Mortazavi, S.; Smart, J. D., An in-vitro method for assessing the duration of mucoadhesion. Journal of Controlled Release **1994,** 31, 207-212.

59. Madsen, F.; Eberth, K.; Smart, J. D., A rheological assessment of the nature of interactions between mucoadhesive polymers and a homogenised mucus gel. Biomaterials **1998,** 19, 1083-92.

60. Di Cola, E.; Yakubov, G. E.; Waigh, T. A., Double-Globular Structure of Porcine Stomach Mucin: A Small-Angle X-ray Scattering Study. Biomacromolecules **2008,** 9, 3216-3222.

61. Georgiades, P.; di Cola, E.; Heenan, R. K.; Pudney, P. D. A.; Thornton, D. J.; Waigh, T. A., A Combined Small-Angle X-ray and Neutron Scattering Study of the Structure of Purified Soluble Gastrointestinal Mucins. Biopolymers **2014,** 101, 1154-1164.

62. Watanabe, Y.; Inoko, Y., Small-angle light and X-ray scattering measurements of a protein-oligosaccharide complex mucin in solution. J Appl Crystallogr **2007,** 40, S209-S212.

63. Waigh, T. A.; Papagiannopoulos, A.; Voice, A.; Bansil, R.; Unwin, A. P.; Dewhurst, C. D.; Turner, B.; Afdhal, N., Entanglement coupling in porcine stomach mucin. Langmuir **2002,** 18, 7188-7195.

64. Yakubov, G. E.; Papagiannopoulos, A.; Rat, E.; Easton, R. L.; Waigh, T. A., Molecular structure and rheological properties of short-side-chain heavily glycosylated porcine stomach mucin. Biomacromolecules **2007,** 8, 3467-3477.

65. Yu, X. Y.; Liu, H. T.; Yang, Y.; Lu, S. Y.; Yao, Q.; Yi, P. G., The investigation of the interaction between Oxymetazoline hydrochloride and mucin by spectroscopic approaches. Spectrochim Acta A **2013,** 103, 125-129.

66. Eftink, M. R.; Ghiron, C. A., Fluorescence quenching studies with proteins. Anal Biochem **1981,** 114, 199-227.

67. Lakowicz, J., Quenching of Fluorescence. In Principles of Fluorescence Spectroscopy, Lakowicz, J., Ed. Springer US: 1999; pp 277-330.